Molecular Biology of the Cell
Vol. 16, 4202–4213, September 2005

The Terminal Phase of Cytokinesis in the *Caenorhabditis elegans* Early Embryo Requires Protein Glycosylation[V]

Huan Wang,* Anne Spang,† Mark A. Sullivan,‡ Jennifer Hryhorenko,* and Fred K. Hagen*

*Department of Biochemistry and Biophysics, Center for Oral Biology and ‡Department of Pediatrics/Immunology/Allergy/Rheumatology, University of Rochester Medical Center, Rochester, NY 14642; and †Friedrich Miescher Laboratory of the Max Planck Society, D-72076 Tuebingen, Germany

Submitted June 1, 2005; Revised June 13, 2005; Accepted June 20, 2005
Monitoring Editor: Reid Gilmore

RNA interference (RNAi) was used to characterize the requirement of protein glycosylation for cell membrane stability during cytokinesis in the early embryo. This screen targeted 13 enzymes or components of polypeptide sugar transferases that initiate either *N*-glycosylation or three different pathways of *O*-glycosylation. RNAi of genes in the mucin-type and epidermal growth factor-fringe glycosylation pathways did not affect cytokinesis. However, embryos deficient in *N*-glycosylation exhibited a variable inability to complete cytokinesis. The most potent block in early embryonic cell division was obtained by RNAi of the polypeptide xylose transferase (ppXyl-T), which is required to initiate the proteoglycan modification pathway. Two generations of ppXyl-T RNAi-feeding treatment reduced the body size, mobility, brood size, and life span of adult animals. Embryos escaping ppXyl-T and Gal-T2 RNAi lethality develop to adulthood but have cytokinesis-deficient offspring, suggesting that glycosyltransferases in the proteoglycan pathway are maternal proteins in the early embryo. Gal-T2::GFP fusions and anti-Gal-T2 antibodies revealed a perinuclear staining pattern, consistent with the localization of the Golgi apparatus. RNAi in green fluorescent protein (GFP)-tagged strains to follow tubulin, PIE-1, and chromatin showed that deficient proteoglycan biosynthesis uncouples the stability of newly formed cell membranes from cytokinesis, whereas cleavage furrow initiation, mitotic spindle function, karyokinesis, and partitioning of intrinsic components are intact.

INTRODUCTION

Cell division, resulting in the formation of two separate daughter cells from one parent cell, is a fundamental requirement for embryonic development and animal life. The later stages of cytokinesis require the coordination of two well-characterized processes. First, a contractile ring of actin and myosin pinches the parent cell, and second, a microtubule network transports membrane vesicles to the cleavage plane of the dividing cell. Vesicle delivery drives the formation of new cell membrane. Mutations in *unc-60*, an actin depolymerizing factor, impair cytokinesis (Ono *et al*., 2003), whereas suppression of either *rab-11* or *syn-4* genes, components of the secretory pathway, results in late stage defects in cytokinesis in *Caenorhabditis elegans* embryos—the cleavage furrow forms, but eventually regresses (Jantsch-Plunger and Glotzer, 1999; Skop *et al*., 2001). The terminal phenotype of mutations in *unc-60*, *rab-11*, and *syn-4* is a multinucleated embryo that continues karyokinesis in the absence of cytokinesis. RAB11 is a GTPase that plays a role in receptor recycling from the endosome to the plasma membrane, and SYN4 is a syntaxin homologue implicated in intracellular organelle and plasma membrane fusion. It has been hypothesized that the mutations in the latter two genes suppress vesicle trafficking, processes that are common to secretion. On a similar theme, brefeldin A (BFA), a potent inhibitor of secretion, blocks membrane vesicle budding, vesicle transport and membrane accumulation at the cleavage plane and also leads to a classic multinucleated phenotype, reflecting a cytokinesis defect (Skop *et al*., 2001).

Membrane vesicles that are affected by these mutations and drugs are potentially derived from an exocytosis pathway or from the Golgi apparatus; therefore, this cytokinesis defect may be the result of a deficiency in secreted and membrane-bound molecules that are normally delivered to the extracellular interface of newly dividing cells (Skop *et al*., 2001). A great deal of emphasis has focused on the importance of membrane vesicle traffic, delivery, and fusion with the plasma membrane (Straight and Field, 2000; Finger and White, 2002), whereas less attention has been placed on the potential cargo inside the vesicles that are delivered to the interface of daughter cells. The contents of the vesicles and their membrane protein components may be important for the stabilization of newly formed membranes in the terminal phase of cytokinesis.

Support for a stabilizing role of secreted material or membrane-associated glycoproteins in cytokinesis mechanisms is provided by studies of the *sqv* genes in *C. elegans*. *Sqv-5* is essential for cell division and has recently been shown by two research groups to synthesize chondroitin, a precursor for the carbohydrate polymers chondroitin sulfate and dermatan sulfate (Hwang *et al*., 2003b; Mizuguchi *et al*., 2003). *Sqv-1* and *sqv-4* genes are essential for the synthesis of

This article was published online ahead of print in *MBC in Press* (http://www.molbiolcell.org/cgi/doi/10.1091/mbc.E05–05–0472) on June 29, 2005.

[V] The online version of this article contains supplemental material at *MBC Online* (http://www.molbiolcell.org).

Address correspondence to: Fred K. Hagen (fred_hagen@urmc.rochester.edu).

Table 1. RNA interference of *C. elegans* protein glycosylation pathways

Cosmid name	Gene name[a]	Initiating enzyme name[b]	Modified amino acid	Linked sugar	Maximal % multinucleated eggs[c] (polyploid in embryos)
N-Glycosylation, activity encoded by genes for multiple subunits					
T22D1.4		OST1, Ribophorin-I	Asparagine	GlcNAc	10 (20)
M01A10.3		SWP, Ribophorin-II	Asparagine	GlcNAc	10 (20)
O-glycosylation, proteoglycan-type. One polypeptide xylose transferase gene					
Y50D4C.4	*sqv-6*	Polypeptide xylose transferase	Serine	Xylose	100 (<1)
O-glycosylation, EGF fringe-type. One polypeptide fucose transferase gene					
C15C7.7		Polypeptide fucose transferase	Serine	Fucose	0 (0)
O-Glycosylation, mucin-type. Nine putative polypeptide GalNAc transferase genes					
ZK688.8	*gly-3*	Polypeptide GalNAc transferase	Ser/Thr	GalNAc	0 (0)
Y116F11B.12	*gly-4*	Polypeptide GalNAc transferase	Ser/Thr	GalNAc	0 (0)
Y39E4B.12	*gly-5*	Polypeptide GalNAc transferase	Ser/Thr	GalNAc	0 (0)
H38K22.5	*gly-6*	Polypeptide GalNAc transferase	Ser/Thr	GalNAc	0 (0)
Y46H3A.6	*gly-7*	Polypeptide GalNAc transferase	Ser/Thr	GalNAc	0 (0)
Y66A7A.6	*gly-8*	Polypeptide GalNAc transferase	Ser/Thr	GalNAc	0 (0)
Y47D3A.23	*gly-9*	Polypeptide GalNAc transferase	Ser/Thr	GalNAc	0 (0)
Y45F10D.3	*gly-10*	Polypeptide GalNAc transferase	Ser/Thr	GalNAc	0 (0)
Y75B8A.9	*gly-11*	Polypeptide GalNAc transferase	Ser/Thr	GalNAc	0 (0)

RNAi by gonad injection of dsRNA, only examined F_1 generation.

[a] The following genes have not occurred in a previous genome-wide RNAi screens: gly-4, gly-5, gly-7, gly-9, gly-10, and gly-11. The Y50D4C.4 RNAi phenotype is reported as wild type by bacterial feeding; T22D1.4 has a low20–40% embryonic lethal RNAi phenotype that does not describe the cytokinesis defect in the genome-wide study (Kamath *et al.*, 2003).

[b] Enzymes initiate specific pathways of protein modification by scanning a protein substrate for a glycosylation site and then catalyzing the transfer of a specific sugar to the protein side chain.

[c] The RNAi screen counted the number of multinucleated eggs that arrest in development at the one- to two-cell stage. Percentage in parentheses indicates the percentage of F_1 that have abnormal multinucleated cells. Values from the plate of F_1 offspring with the highest penetrance are shown.

UDP-xylose and *sqv-7* transports multiple-nucleotide sugars to the endoplasmic reticulum (ER)/Golgi. Null mutations in *sqv-1* and *sqv-7* result in progeny that fail to initiate cytokinesis (Hwang and Horvitz, 2002). These latter gene products (SQV-1, SQV-4, and SQV-7) provide substrates for glycosylation reactions that posttranslationally modify diverse classes of secreted and membrane-bound glycoconjugates.

To examine multiple protein glycosylation pathways, our study reported here identified all the polypeptide sugar transferases known in *C. elegans* and conducted an RNA interference (RNAi) screen. Many of these genes have not been examined in previous genome-wide RNAi studies. Polypeptide sugar transferases are the key enzymes that initiate specific protein glycosylation pathways by recognizing protein substrates and then modifying their amino acid side chains with specific sugar residues. In *C. elegans*, the glycosylation machinery is similar to that in mammals in that nematodes express glycosyltransferase enzymes found in both *N*-linked and *O*-linked glycosylation pathways (Table 1). In this study, we used RNAi to examine the impact of 13 *C. elegans* glycosyltransferase genes on cytokinesis in the developing *C. elegans* embryo. The penetrance of the RNAi phenotype was dependent on the duration of RNAi treatment. Continuous bacterial feeding RNAi for two generations permitted the analysis of maternal-effect lethal phenotypes. Glycosyltransferases in the pathway that were most critical for cytokinesis were cloned and expressed to validate their function and to develop single-chain antibodies. Antibodies and green fluorescent protein (GFP) reporter constructs were used to analyze the subcellular localization of the glycosyltransferase and the properties of glycosyltransferase-deficient embryos.

MATERIALS AND METHODS

Cloning, Expression, and Purification of Glycosyltransferases

cDNAs for *C. elegans* pXyl-T (Y50D4C.4) were amplified using PRIM-1 d[CGCGTCGCATATTTCGTCGGATAG] and PRIM-69 d[CTCCGGAGCG-GCCGCTAAATCAAGGTCTGCGTATC]. An intact Gal-T2 cDNA was ob-

tained from the expressed sequence tag clone yk0292g2 and was amplified with the primers PRIM-118 d[CGCGTCACCGCCAGCAACACCTTCAGCCATCA] and PRIM-143 d[GTGCGGCCGCTGGATTCTAATACGACTCACTATAGGG]. The soluble catalytic domains encoded by these cDNA fragments were ligated into the MluI and *Not*I sites of pS2-MKF3c, an S2 cell expression vector with a low copy origin of replication and a purification tag sequence from pIMKF3 (Hagen and Nehrke, 1998).

The pS2-MKF3c vector uses a signal peptide to direct the secretion of N-terminal purification (metal chelate and FLAG epitope) tags fused to the cDNA coding regions, described above. *Drosophila* S2 Schneider cells were cotransfected with pCo-BLAST and placed under blastocidin selection for 4–12 wk, as described by the supplier (DES system; Invitrogen, Carlsbad, CA). Recombinant protein expression was induced from the metallothionein promoter by adding 650 μM copper sulfate. After 5 d, the culture media were harvested and was buffer exchanged, using a 10-kDa molecular mass cut-off membrane filter and a Pellicon tangential flow system (Millipore, Billerica, MA). The secreted, recombinant protein was purified, using metal chelate chromatography on Talon resin (BD Biosciences Clontech, Palo Alto, CA) and anti-FLAG M1-agarose resin (Sigma, St. Louis, MO), using the protocols recommended by the manufacturers. Protein yield and purity was determined by silver staining on SDS-PAGE and by Western blot analysis.

Anti-Gal-T2 Antibody Production

An antibody-phage display method was used to isolate recombinant antibodies that bind to Y110A2AL.14, the *C. elegans* Gal-T2 protein. Recombinant antibodies were obtained from a library of human single-chain variable antibody fragments (scFv), fused to M13 gene III (Haidaris *et al*., 2001). A panning procedure was used to enrich for tight-binding clones. Briefly, recombinant Gal-T2 was immobilized at a concentration of 10 to 50 μg/ml in Tris-buffered saline (TBS) to Nunc Immunoplates and then blocked in 0.5% Blocker Reagent (Roche Diagnostics, Indianapolis, IN) in TBS. Then, 10^{12} human scFv antibody-phage was incubated with the immobilized antigen for 2 h at room temperature. Unbound phage was removed by washing with TBS plus 0.5% Tween 20 (TBST). Bound phage was eluted in 50 μl of freshly prepared 100 mM glycine-HCl, pH 2.2, with 1 mg/ml bovine serum albumin (BSA). Eluted phage was neutralized with 3 μl of 2 M Tris-free base, transduced into TG1 host cells, and infected with M13VCS helper phage to generate phage for the next enrichment. The panning protocol was repeated for a total of three enrichments and individual clones of tight-binding phage were identified by an enzyme-linked immunosorbent assay (ELISA). Positive clones were treated with *Sal*I and *Xho*I to delete the M13 gene III coat protein, to produce soluble scFv proteins with an N-terminal FLAG epitope tag and a C-terminal His_6 tag. Anti-Gal-T2 scFv protein was produced by growing scFv constructs under low phosphate conditions, and protein was purified from the *Escherichia coli* host BL21 codon plus (Stratagene, La Jolla, CA) using BugBuster (Novagen, Madison, WI) and metal chelate chromatography on Talon resin (BD Biosciences Clontech). Final recombinant scFv protein was dialyzed against 100 mM NaCl, 20 mM 2-(*N*-morpholino)ethanesulfonic acid [MES], pH 6.5, and stored at −80°C. The anti-Gal-T2 scFv antibody works in both ELISA and Western blot detection and is specific for the Gal-T2 protein and not the fusion tag.

Detection and Localization of Gal-T2 Protein

To evaluate antibody specificity, the following protein preparations were probed by Western blot: 1) 1–50 ng of recombinant Gal-T2 fused to a 38-aa FLAG epitope-metal chelate tag; and 2) recombinant Gal-T2 cleaved from the 38-aa tag, using human rhinovirus 3c protease. For subcellular localization, mixed stage N2 *C. elegans* nematodes were fixed and incubated with anti-Gal-T2 antibodies. Briefly, worms and embryos were 1) fixed in fresh 4% paraformaldehyde; 2) permeabilized at 4°C in 1% Triton X-100, 100 mM Tris, pH 7.4; and 3) reduced at 37°C in 1% β-mercaptoethanol, 1% Triton X-100, 100 mM Tris, pH 7.4, for 60 min at each step (Nonet *et al*., 1993). These specimens were then treated with 10 mM $NaBO_3$, 0.3% H_2O_2 for 1 h at room temperature, and then placed in Blocker solution (phosphate-buffered saline [PBS], 0.5% Triton X-100, 0.05% Na-azide, 1 mM EDTA, and 0.1% BSA) plus 1% BSA. For antibody incubations, animals were washed in Blocker solution and were treated sequentially with a series of antibodies: anti-Gal-T2 scFv antibody, mouse anti-FLAG M2 antibody (Sigma), and a goat anti-mouse IgG antibody (Molecular Probes, Eugene, OR), by incubating each antibody in Blocker solution at 37°C for 1 h. Animals were mounted for microscopy with an equal volume of Vectashield (Vector Laboratories, Burlingame, CA).

Gal-T2::GFP Reporter Constructs

Prim241 d[ACAAACACCCGCCTGTGCCTGTCAATCT] and Prim242 d[TTTAGCGCCACCCTGTCCCAGAAATGTTTCGGGAAGATTAGTTG] were used to amplify Gal-T2 genomic sequences, which include 2.4 kb of 5′ untranslated region (UTR), exon 1, intron 1, part of exon 2, and the 18-nucleotide (nt) PCR-fusion linker sequence. A GFP-encoding fragment was amplified from pPD122.15, containing (from upstream to downstream end) an 18-nt PCR fusion linker, GFP(S65C), four synthetic introns, and let-858 3′UTR, using primers Prim172 d[GGACAGGGTGGCGCTAAACAGGACCCAAAGGTATGTTTC] and Prim156 d[TACAGACAAGCTGTGACCGTCTCC]. The Gal-T2 gene fragment was fused at amino acid 60 of Gal-T2 to the N terminus of GFP, using the Expand 20-kb Plus PCR system (Roche Diagnostics), Prim244 d[GGAGACTGCTATCAAGAATCGGTATGG], and Prim157 d[CGGGAGCTGCATGTGTCAGAGGTT]. This construction positioned GFP after the putative Golgi transmembrane anchor, targeting GFP to the lumen of the Golgi. The Gal-T2::GFP reporter construct was coinjected with wild-type *pha-1* gene into the gonads of the worm strain GE24. Transgenic animals were selected at 23°C.

Glycosyltransferase Assays

Recombinant glycosyltransferases were incubated at room temperature for 1–4 h in a 25-μl reaction volume containing 25 mM MES, pH 6.5, 25 mM KCl, 5 mM KF, 5 mM $MgCl_2$, and 5 mM $MnCl_2$. For xylosyltransferase activity, the following reaction substrates were added: UDP-[^{14}C]xylose (20,000 cpm) and the biotinylated peptide based on the human bikunin proteoglycan glycosylation site, NH_2-GEEEGSGGGQKK(biotin)-COOH (Alpha Diagnostic, San Antonio, TX). To separate the radiolabeled glycopeptide reaction product, the reaction was mixed with 25–50 μl of an 1:1 slurry of streptavidin-agarose in PBS and incubated for 30 min. The unincorporated label was washed from the streptavidin beads two times, by adding 500 μl of PBS, containing 0.1% Triton X-100, and centrifuging the beads for 5 s at 5000 rpm in a Microfuge. Substrates for galactosyltransferase assays include UDP-[^{14}C]galactose and various sugar acceptor analogues, chemically coupled to benzyl groups (Sugaris, Muenster, Germany). Galactosyltransferase reaction products were separated by anion exchange chromatography, using AG 1x8 resin (Bio-Rad, Hercules, CA). Glycosyltransfer reaction controls to test for nucleotide sugar hydrolysis included 1) assays in the absence of the sugar acceptor or 2) assays that used Gal-β-biotin substrate and streptavidin-agarose separations. No sugar-nucleotide hydrolysis was observed.

Worm Culture

Wild-type N2 and a RNAi hypersensitive mutant NL2099 were cultivated on NGM agar plates seeded with OP50 *E. coli*. Animals were well fed on an OP50 food source for a minimum of two generations and never allowed to starve before and during RNAi treatment. The following GPF-tagged nematode strains were cultivated in an identical manner: AZ212 for histone::GFP, WH204 for tubulin::GFP, and JH227 for Pie-1::GFP.

Microscopy

Animals were initially examined and scored, using a stereomicroscope. For time-lapse microscopy, embryos were dissected from gravid adults, mounted on an agar pad and imaged, using a Nikon E800 upright microscopy with motorized shutters and Z-axis focus or an Axioplan 2 equipped with an Axiocam (Carl Zeiss, Oberkochen, Germany). Time-lapse and Z-focus recordings were acquired every 20–30 s, using the SimplePCI software (Compix, Cranberry Township, PA) and a SPOT2 digital camera.

RNA Interference Methods

Double-stranded RNA (dsRNA) Injection. Individual cDNAs (*apx-1*, GFP, *unc-54*, Gal-T2, and ppXyl-T) were PCR amplified with primers that contain T7 RNA polymerase promoter sites on the 5′ end of both the upstream and downstream primers. RNA was produced using 100 ng of the PCR product in a 10-μl in vitro transcription reaction using Megascript (Ambion, Austin, TX). dsRNA was annealed by a 2-min 90°C denaturation step, followed by slow cooling to 30°C over a 30-min period. The dsRNA was ethanol precipitated and resuspended to a final concentration of 1–5 mg/ml. Young adults were injected in a single gonad, and, after a 4- to 8-h recovery period, healthy adults were transferred individually to fresh OP50 plates every 24 h for 3 d. The embryonic lethality rate was calculated 12–14 h after the adult was removed from the plate.

RNA Interference by Bacterial Feeding. Gal-T2, ppXyl-T, and *unc-54* cDNAs were cloned into the vector pPD128.36 (Timmons *et al*., 2001) and then transferred to the *E. coli* strain HT115, which was grown to mid-log phase in liquid culture, induced with 1 mM isopropyl β-D-thiogalactoside (IPTG) for 1 h, and plated at a 5× concentration at 23°C for one night, either on IPTG-NGM agar (Kamath *et al*., 2003) or on lactose plates. For lactose-induced RNAi, lactose plates were prepared, containing 2% agar, 0.5% casamino acids, 0.2% lactose, 0.1% NH_4Cl, 0.05% NaCl, 1× M9 buffer, 1 mM $CaCl_2$, 0.0005% cholesterol, and 200 μg/ml ampicillin. Worms were seeded on the induced lawn and incubated at 23°C. No more than four worms were added to any one plate, or else the RNAi induction did not work. Animals were cultured for 1 to 2 d and transferred to fresh plates. F_1 progeny that escaped lethality of RNAi treatment were seeded on new RNAi plates for a second generation of bacterial feeding.

Quantitative Reverse-Transcription PCR

Total RNA template was isolated from staged worm or embryo samples in 300 μl of Tri Reagent and 2 μl of polyacrylamide carrier (Molecular Research Center, Cincinnati, OH). For RNAi-treated embryos, at least 20 embryos were

used for RNA isolations. First-strand cDNA synthesis was conducted using Super Script III (Invitrogen) in a final volume of 20 μl, including either 2.5 μg of total RNA or RNA from an equivalent of 5 embryos. For PCR quantitation, 0.25 μl of staged cDNA or 1 μl of the 20-embryo cDNA preparation was used as a template. PCR reactions were conducted in a Bio-Rad iCycler in 25-μl reactions, using 12.5 μl of iQ-SYBR Green Super Mix and 0.4 μM oligos. PCR primers for Gal-T2 cDNA are Prim613 d[ATCCGAGATTTGATACCGAATGGAGA] and Prim614 d[ACGTAGGATGGATGTTTTTGGAACTC]. PCR primers for a cDNA control (*ama-1*) are Prim610 d[ACGTTGAAAAAGGTAACATGCAATACA] and Prim612 d[GAAGCCATGGAGAGGTACGCGATAGAT]. At least one oligo in each pair was designed around splice junctions to avoid genomic DNA contamination. All reactions were performed in triplicate and a standard curve with a 4 or 5 log dilution series was used. Negative controls, lacking templates, were included on all sample runs. The relative copy number of the Gal-T2 template was normalized to either the total RNA template concentration or the *ama-1* template copy number. All experimental values fell within the range of the standard curve.

RESULTS

RNAi Screen of the Major Protein Glycosylation Pathways

An RNAi screen was used to determine which glycosylation pathways are most critical for cytokinesis and preventing cleavage furrow regression. The phenotypic readout of the assay was the observation of multinucleated eggs or abnormal polyploid cells in early embryos. This screen, therefore, selects for glycosyltransferases that are essential for cell membrane stability during cytokinesis in the early embryo, whereas other cellular functions, such as mitotic spindle formation and karyokinesis, are normal. During the course of experiments, we found that the mode and duration of dsRNA delivery had a great impact on the effectiveness of RNAi treatment targeted against glycosyltransferase gene products. Bacterial feeding RNAi was significantly more effective with lactose plate dsRNA induction, compared with the traditional IPTG plate induction. RNAi via injection of dsRNA, although more labor-intensive, was more potent in the F_1 generation and thus used in the initial screen and identification of critical glycosyltransferases.

To ensure that multiple protein glycosylation pathways are addressed in an RNAi screen, we identified the key glycosyltransferase genes in all known protein glycosylation pathways that modify proteins in the secretory pathway, either based on sequence similarity with known mammalian glycosyltransferases or from nematode enzymes that have been functionally expressed in previous reports. A total of 13 *C. elegans* glycosyltransferase gene products were targeted for RNAi knockdown analysis (Table 1). Three genes in our study (Y50D4C.4, M01A10.3, and T22D1.4) produced an embryonic lethal phenotype by dsRNA injection, whereas a previously published bacterial-feeding RNAi study including these genes showed a weak or wild-type phenotype (Kamath *et al*., 2003).

The first gene targets described in Table 1 include some of the critical components of the oligosaccharyltransferase (OST) complex, which initiates *N*-glycosylation. Little experimental information has been reported on the *N*-glycosylation machinery in *C. elegans*. Protein *N*-glycosylation is initiated by a multiprotein, membrane-bound OST complex, which scans for *N*-glycosylation sites on newly synthesized proteins, during protein translation and translocation into the endoplasmic reticulum. Protein sequence analysis suggests that there are seven *C. elegans* candidate proteins that either make up the OST complex or are involved with the assembly of the complex. T22D1.4 encodes for a putative 586-aa type-1 membrane protein, representing the *C. elegans* OST1/ribophorin-1 subunit, which is important for assembly of the OST complex, is positioned close to the substrate binding site, but it is not directly involved with substrate recognition or catalysis (Yan and Lennarz, 2005). OST1 is required for *N*-glycosylation in yeast and essential for viability (Knauer and Lehle, 1999). RNAi of T22D1.4 resulted in 70% embryonic lethality, where development was arrested at multiple stages (Table 1). Between 2 and 10% of the arrested T22D1.4 RNAi-treated embryos exhibited a multinucleated phenotype, a cytokinesis defect at the one- to two-cell stage, whereas 20% of embryos arrested with some polyploid cells. Another subunit of the OST complex is the SWP protein, or ribophorin-II, which copurifies with OST1 from yeast and is required for full OST activity in yeast (Knauer and Lehle, 1999). The *C. elegans* protein M01A10.3 has a membrane topology and sequence motif structure that is identical to the yeast and mammalian SWP/ribophorin-II protein (Krogh *et al*., 2001; Bateman *et al*., 2004). RNAi of *C. elegans* ribophorin-II demonstrated a loss-of-function phenotype that was identical to that of ribophorin-I (Table 1). A similar phenotype and penetrance (our unpublished data) was observed for RNAi targeted at other subunits of the OST complex, OST2/dad-1 and STT3, a subunit which plays a critical role in catalysis of *N*-glycosylation in yeast (Yan and Lennarz, 2005). In summary, our RNAi analysis of *C. elegans* OST subunits showed a consistent cytokinesis defect that led to a variable-stage developmental arrest, which was not described in previous genome-wide RNAi screens.

To examine diverse protein *O*-glycosylation pathways in the context of cytokinesis, gene targets for polypeptide sugar transferases in the proteoglycan, epidermal growth factor (EGF)-fringe, and mucin-type modification pathways were identified. In contrast to *N*-glycosylation, polypeptide sugar transferases in *O*-glycosylation pathways are monomeric Golgi enzymes that scan proteins for specific amino acid sequence motifs that define glycosylation sites and catalyze the transfer of a specific monosaccharide to a serine or threonine hydroxyamino acid in the motif. The initiating enzymes in each of the three protein *O*-glycosylation pathways function independently, as a single enzyme species. The first monosaccharide attached to the protein side chain is unique for each modification pathway (xylose in proteoglycans, fucose in EGF repeats, and GalNac in mucin glycoproteins), and subsequently these attached monosaccharides become substrates for downstream glycosyltransferases to build oligosaccharide structures unique for each glycosylation pathway.

The RNAi screen, targeting 11 genes in *O*-glycosylation pathways, demonstrated that early embryonic defects are prevalent in embryos deficient in polypeptide xylose transferase (ppXyl-T), Y50D4C.4 (Table 1 and Figure 1). Only some of the ppXyl-T RNAi-injected animals produced F_1 progeny with a cytokinesis defect. For these affected animals the initial brood was wild-type; however, when the multinucleated phenotype occurred (2–3 d postinjection), most siblings on the same plate shared the same cytokinesis defect. Some F_1 progeny escaped the ppXyl-T RNAi treatment; however, at adulthood, they exhibited an egg-laying defect and were bloated with multinucleated embryos (Figure 1D). This maternal-effect phenotype is surprising because RNAi is potent for depleting both maternal and zygotic mRNA. The most plausible explanation for surviving ppXyl-T RNAi F_1 animals, carrying F_2 embryos with a cytokinesis arrest, is that the maternal component needed for the first cell divisions in the early embryo is a protein (the glycosyltransferase enzyme) that is stored in oocytes. ppXyl-T (Y50D4C.4 or SQV-6) is the only *C. elegans* protein with sequence similarity to the two human polypeptide xylose transferases (Gotting *et al*., 2000; Hwang *et al*., 2003a); therefore, the

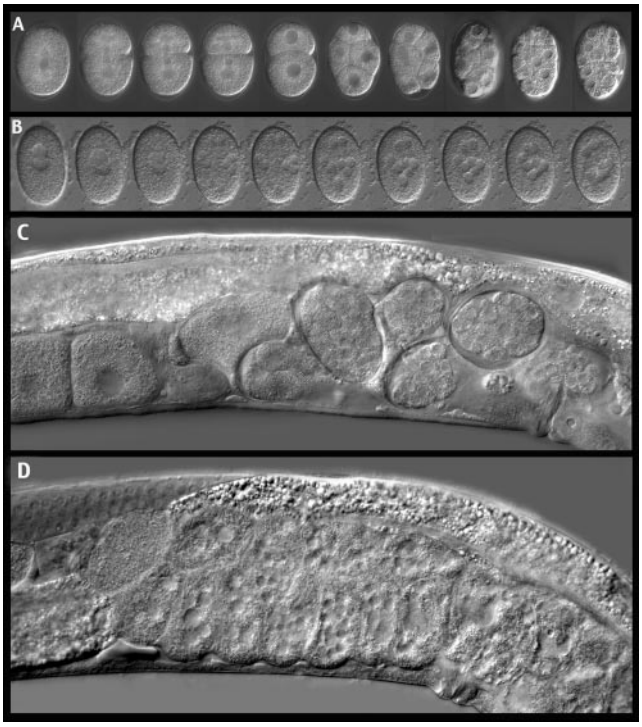

Figure 1. ppXyl-T RNAi impairs cytokinesis and leads to an egg-laying defect, multinucleated embryos, and embryonic arrest. A time-lapse panel demonstrates normal cell division in the early *C. elegans* wild-type embryo (A) and the development of multinucleated embryos after ppXyl-T RNAi treatment (B). (C) N2 oviduct and uterus of a gravid wild-type adult. (D) ppXyl-T RNAi results in an egg-laying defective adult, which is packed with multinucleated embryos that exhibit defects in early embryo cytokinesis.

Y50D4C.4-deficient embryos suggest that proteoglycan-type modification is essential for early embryonic development.

To perform a similar loss-of-function analysis with EGF-fringe protein glycosylation, RNAi was targeted to C15C7.7 gene, the only candidate polypeptide fucose transferase in *C. elegans*. Polypeptide fucose transferase attaches fucose to EGF repeats. Very little is known about EGF-fringe glycosylation in nematodes, whereas in *Drosophila* EGF-fringe glycosylation is essential for modulating notch receptor-ligand interactions. Using dsRNA injection, C15C7.7 showed a wild-type phenotype in the context of cell division in early embryos.

RNAi also was used to down-regulate enzymes that initiate mucin-type *O*-glycosylation. In contrast to proteoglycan, EGF-fringe and *N*-glycosylation pathways, mucin-type *O*-glycosylation is initiated by a large family of 13 independent polypeptide GalNAc transferase isoforms. Eleven *C. elegans* polypeptide GalNAc transferases have been expressed as recombinant proteins, and five of these isoforms are functionally active with mammalian mucin peptide substrates (Hagen and Nehrke, 1998). cDNA cloning and genome sequence analysis indicate that a total of 13 polypeptide GalNAc transferases are encoded by nine genes, designated as *gly-3*, *-4*, *-5*, *-6*, *-7*, *-8*, *-9*, *-10*, and *-11*, in which *gly-5* and *gly-6* are alternatively spliced into three isozymes, each (Hagen *et al*., 2001). The size of the *C. elegans* polypeptide GalNAc transferase family is smaller than that of mammals, which is predicted to include up to 24 members. RNAi of the individual *gly-3* through *gly-11* genes did not result in an early arrest in embryonic development (Table 1). It is possible that gene redundancy may mask loss-of-function phenotypes in our RNAi analysis. To address gene redundancy issues, we injected more than one *gly* dsRNA at one time, yet we did not observe an early embryonic arrest. In addition, we used a transgene construct to express different combinations of five to nine *gly* antisense RNAs at one time, but we also did not observe an early embryonic arrest phenotype. It is possible that injection of mixtures of dsRNA or expression of antisense RNA from transgenes has limited effectiveness in the early embryo.

Cell Membrane Behavior in Early ppXyl-T-deficient Embryos

To examine the loss-of-function phenotype of *C. elegans* ppXyl-T in greater detail, the Y50D4C.4 mRNA was depleted by RNAi and observed by time-lapse microscopy (Figure 1). Time-lapse microscopy of ppXyl-T-deficient embryos shows that the cleavage furrow forms but does not progress to completion (Movies M1 and M2). Eventually, these stalled cell membranes (in the cleavage plane) collapse back to the cell membrane encompassing the embryo, as the next round of nuclear division is initiated. As nuclear divisions progress, the plasma membrane expands to fill the entire eggshell. The properties of the plasma membrane or the membrane–eggshell interactions seem to be altered, because ppXyl-T RNAi fertilized eggs filled out the eggshell entirely, whereas in wild-type embryos there was a space, especially in the anterior where the polar bodies were extruded (compare Figures 1, A and B, and 2A). Time-lapse microscopy also showed that membrane dynamics in the anterior of the ppXyl-T-deficient embryos were different from wild-type embryos. In wild-type embryos, plasma membrane ruffling and blebbing is very active on the anterior cell surface of the anterior embryo (the AB cell), which develops transient ectopic cleavage furrows that were unproductive and rapidly regressed into the original cell surface. This transient membrane blebbing is normal in the wild-type embryo, but it is exaggerated as more stable ectopic cleavage furrows in *mel-11* mutants, which is a gene that regulates the rate of nonmuscle myosin contractions, involved in cleavage furrow progression (Piekny and Mains, 2002). In the ppXyl-T-deficient embryos, however, the transient membrane blebbing and ectopic cleavage furrow formation on the anterior surface of the AB cell was completely absent (Figures 1, A and B, and 2A and Movies M1 and M2).

The ppXyl-T RNAi treatment also rendered the embryos susceptible to cell lysis, as the embryos easily disrupted through the eggshell upon handling. Eggs laid by ppXyl-T RNAi-treated adults also had a flattened appearance and degraded rapidly on the agar plate. Collectively, the loss of rounded cell shape and extracellular space and the disappearance of normal membrane furrowing suggest that the biosynthesis of proteoglycans support the cell membrane structure and stabilize normal changes in cell shape during cytokinesis.

Nuclear Divisions, Mitotic Spindles, and Partitioning in ppXyl-T-deficient Embryos

To determine whether proteoglycans affect membrane–cytoskeleton interactions, the position of the spindle apparatus, and embryo polarity, we next examined the properties of glycosyltransferase-deficient embryos, using GFP-tagged marker proteins (Figure 2 and Movies M1 and M2). In ppXyl-T RNAi-treated embryos, tagged with histone::GFP, the timing of the first two rounds of nuclear divisions seemed normal, even in the absence of complete cytokinesis (Figure 2A). The cleavage plane and midbody were posi-

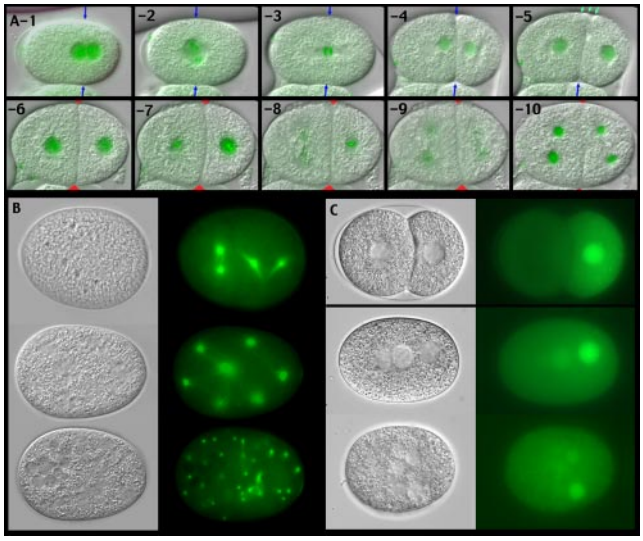

Figure 2. ppXyl-T RNAi of embryos with GFP-tagged marker proteins demonstrates normal spindle behavior and partitioning properties at the first and second nuclear divisions. (A) Histone::GFP shows normal karyokinesis and a normal initiation of cytokinesis. The spindle is asymmetrically positioned (blue arrows). When cytokinesis is nearly complete, the cleavage furrow begins to regress (green arrows) and an intercellular bridge forms. The daughter cells then loose their rounded shape, whereas the cleavage furrow completely disappears (red arrows). Significantly more cell membrane disappears from the cleavage plane, whereas the spindle apparatus duplicates and begins to initiate the next round of nuclear division. (B) tubulin::GFP shows that the spindle is actively duplicating, migrating and initiating karyokinesis, in the absence of proteoglycans in ppXyl-T RNAi-treated embryos. Centrosome duplication occurs and the microtubule arrays interdigitate (C) PIE-1::GFP of a normal two-cell embryo (top) and in ppXyl-T RNAi-treated embryos (bottom two panels). The PIE-1::GFP signal is present in the most posterior nucleus. Embryos are orientated so that anterior is to the left.

tioned correctly in P_0, to the posterior, such that the AB daughter is larger than the P_1 daughter. Cleavage furrow formation initiated like normal. However, at the time cytokinesis was nearly complete, daughter cell separation began to collapse: the intracellular bridge along the cleavage plane expanded and the cleavage furrow regressed. The second round of nuclear divisions commenced with staggered timing, as expected in normal embryos (AB nuclei divides before P_1). However, when the second round of cytokinesis should have begun to form four cells, the remaining cell membrane from the first cleavage plane began to diminish. ppXyl-T RNAi of tubulin::GFP tagged embryos showed that the spindle apparatus behaved normally, as, in most cases, mitotic spindles were asymmetrically positioned at the first nuclear division and karyokinesis progressed normally. The P_1 spindle rotated and set up normal perpendicular segregation planes in the absence of new cell membrane (Figure 2B, top), but proper spindle orientation was not consistent, because, in some cases, the chromosome segregation planes were parallel for the AB and P_1 cells (Figure 2A, 10). In subsequent nuclear divisions, the centrosomes duplicated normally, but because of the absence of cellularization, the microtubules from different arrays interdigitated and many nuclei eventually clumped in the center of the embryo (Figure 2B, bottom). Also, in normal embryos, an intact cell membrane of AB daughter cells is required to allow one AB daughter to slide anterior to its sister cell. After the second round of nuclear divisions, in the ppXyl-T RNAi embryos, the AB daughter nuclei divided across the embryo's transverse axis but did not reposition along the anterior-posterior axis because separate AB daughter cells do not form and slide past one another. As a result, the subsequent nuclear positions were not normal in ppXyl-T-deficient embryos.

PIE-1::GFP embryos were used to determine whether the polarity of the early embryo was lost upon failure to complete cytokinesis in ppXyl-T-deficient embryos. Wild-type embryos showed PIE-1::GFP concentrated in the posterior nucleus in the P_1 cell (Figure 2C, top), and, in later-stage embryos, PIE-1 accumulation was retained in the P-lineage. The polarity of this protein distribution was not lost in ppXyl-T-deficient embryos. Even though cytokinesis failed in ppXyl-T RNAi embryos, PIE-1::GFP accumulated in only one nucleus, which was in the posterior embryo (Figure 2C, middle and bottom). These results indicate that, although the plasma membrane structure was affected in ppXyl-T RNAi embryos, the spindle apparatus position, orientation, and timing was normal most of the time and the embryo's polarity cues remained in place.

Analysis of Recombinant Glycosyltransferases from the Proteoglycan Pathway

To determine whether glycosyltransferases were present in the early embryo, we attempted to overexpress all glycosyltransferases in the proteoglycan biosynthesis pathway and produce antibody probes. Recombinant ppXyl-T protein was positive for xylose transferase activity, but the protein yield was insufficient for an antibody screen. Antibodies could only be produced for Gal-T2 (Y110A2AL.14), because all other glycosyltransferases were refractory to expression. Gal-T2 adds the third sugar in the proteoglycan linker tetrasaccharide (Figure 3). Y110A2AL.14 or SQV-2 is a member of a large family of 21 *C. elegans* proteins with sequence similarity to β1,3-galactosyltransferases; however, Y110A2AL.14 has significantly higher sequence similarity with mammalian Gal-T2 than with any other worm galactosyltransferases, suggesting that there is only one nematode gene that encodes for Gal-T2 activity.

To select for antibodies against a functional Gal-T2 protein, first a recombinant Y110A2AL.14 protein was expressed in high yield in *Drosophila* S2 insect cells and examined for enzyme activity, before antibody production. Numerous sugar substrates were tested, because Y110A2AL.14 has significant amino acid sequence similarity with multiple galactosyltransferases in different glycosylation pathways (Figure 3, A and B). Although no transfer of galactose was catalyzed to monosaccharide acceptor substrates ending with GalNAc, GlcNAc, fucose, and xylose, Y110A2AL.14 protein did glycosylate Gal-terminating sugar analogues. Higher activity was observed with an acceptor substrate that had a galactose in a β-linkage, suggesting that the enzyme binds galactose substrates, but it is sensitive to configuration of groups attached to galactose (Table 2). The highest rate of transfer was observed for the substrate Gal-β1,4-Xyl-β-Bz, indicating that Y110A2AL.14 has approximately a 2000-fold greater specificity for this xylose containing sugar, which is a biosynthetic intermediate (see single-underlined sugars) of the proteoglycan tetrasaccharide linker: GlcA-β1,3-**Gal-β1,3**-Gal-β1,4-Xyl-1β-O-serine-(protein). The highly selective specificity of this recombinant protein indicated that Y110A2AL.14 is Gal-T2, the galactosyltransferase that adds the second galactose (see double underline) to tetrasaccharide linker of proteoglycans: GlcA-**Gal**-Gal-Xyl-O-serine. Furthermore, Y110A2AL.14 is only capable of galactose transfer activity, as no transferase activity was detected with

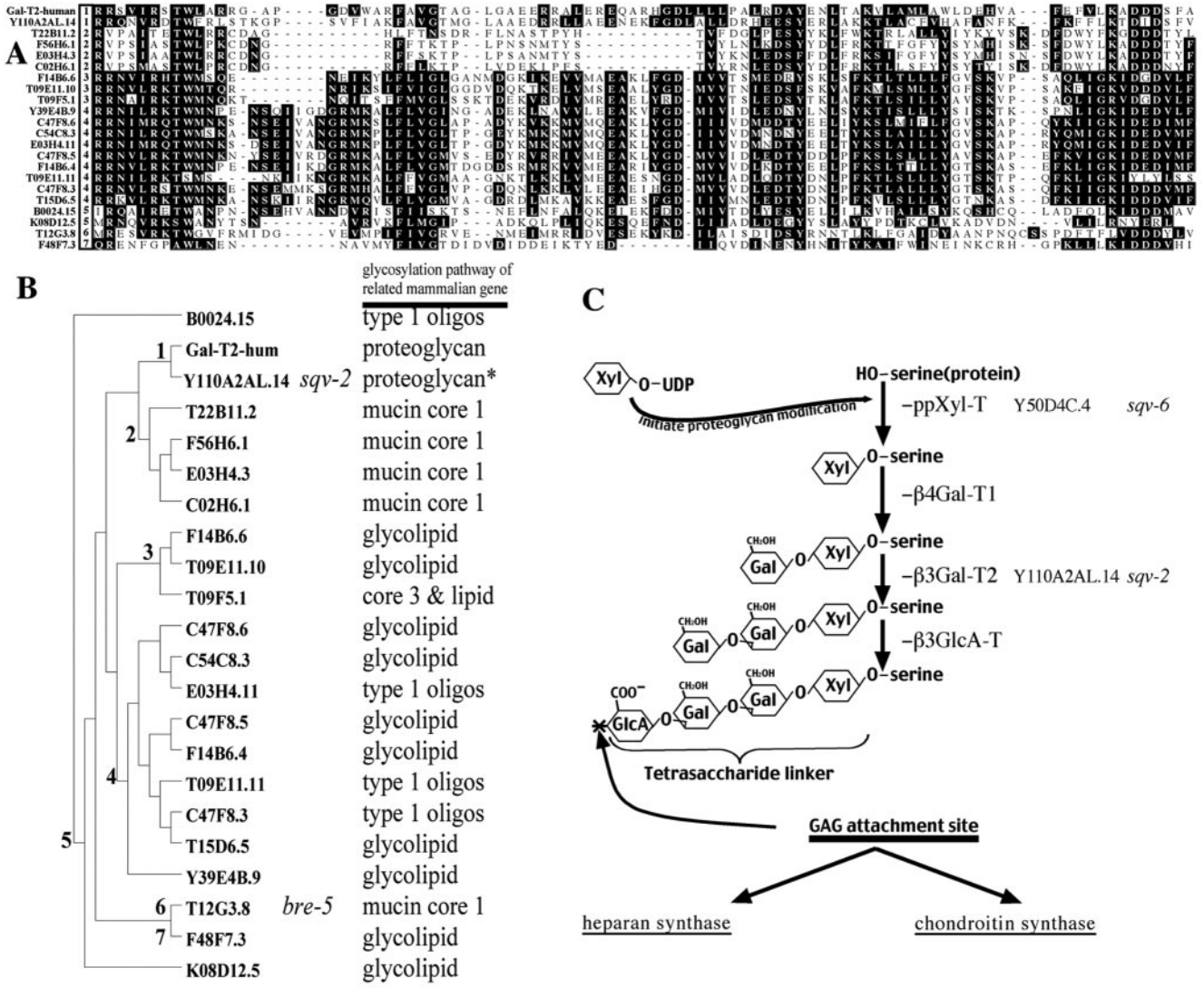

Figure 3. Y110A2AL.14/SQV-2 is a member of the β1,3 Gal-T family in *C. elegans*. (A) Amino acid sequence alignments of the sugar-donor substrate-binding site of 21 putative *C. elegans* β1,3 Gal-T proteins and the human Gal-T2 protein. (B) Phylogenetic analysis based on this catalytic domain, shown above. Annotations list the glycosylation pathway of the most closely conserved mammalian sequence homologue for each worm gene. Type-1 oligos refers to type-1 Galβ1,3GlcNAc-R oligosaccharides. The actual sugar structures that are synthesized by most of these enzymes are not known, but they fall in a family of sugars with a β1,3-linkage. (C) Gal-T2 is in the proteoglycan biosynthesis pathway. The pathway begins with an initiation reaction, the transfer of xylose to a serine residue in a proteoglycan, by ppXyl-T. A tetrasaccharide linker (GlcA-Gal-Gal-Xyl-serine) is built through the sequential action of individual glycosyltransferases that add one sugar at a time, after the xylose modification of peptide sequences has occurred. *C. elegans* Gal-T2 is encoded by Y110A2AL.14 or *sqv-2* and is a galactoslytransferase that specifically adds the third sugar residue in the linker tetrasaccharide. Gal-T1 and GlcA-T are encoded by the *sqv-3* and *sqv-8* genes, respectively. Glycosaminoglycan (GAG) chains chondroitin and heparan biosynthesis require the tetrasaccharide linker.

other nucleotide sugars (Table 2). The observations, described here, confirm and expand on the enzyme activities reported on SQV-2 (Hwang *et al*., 2003a).

Kinetic analysis with the purified recombinant Y110A2AL.14 protein provided a Km(UDP-Gal) value of 103 μM and a Km(Gal-Xyl-Bz) of 180 μM. Parallel assays run in the presence of 5 mM Gal-β-Bz had no effect on either the K_m or V_{max}, indicating that a related or pseudosubstrate, Gal-β-Bz, is not an effective competitive inhibitor of Gal-T2. Therefore, cross-talk or pseudosubstrate inhibition with other glycosylation pathways is likely to be rare, even though numerous galactose-terminating oligosaccharide intermediates coexist in the Golgi apparatus and even though the Y110A2AL.14 active-site is capable of docking with simple α-linked and β-linked galactose analogues. This functional preparation of recombinant Gal-T2 was used to screen a single-chain antibody library.

Localization of Proteoglycan Gal-T2 Enzyme in C. elegans

A single-chain Fv antibody (scFv) against Y110A2AL.14 protein was obtained from a library of 10^9 unique antibody-phage. This antibody reacted both with the functional antigen in ELISA and with the denatured antigen on a Western blot. The anti-Gal-T2 scFv showed a strong immunofluorescence signal in all cells of early and late embryo specimens, revealing numerous punctate organelles surrounding the nucleus (Figure 4, A–C, and Movie M3). Nuclei were always

Table 2. Y110A2AL.14 protein exhibits proteoglycan Gal-T2 activity

Sugar donor	+	Acceptor	↔	nt	+	Glycosylated product	Reaction rate (pmol/h)[a]
10 μM		5 mM					
UDP-Gal	+	GalNAc-β-Bz	↔			No product	0
UDP-Gal	+	GalNAc-α-Bz	↔			No product	0
UDP-Gal	+	GlcNAc-β-Bz	↔			No product	0
UDP-Gal	+	GlcNAc-α-Bz	↔			No product	0
UDP-Gal	+	Fuc-α-Bz	↔			No product	0
UDP-Gal	+	Xyl-β-Bz	↔			No product	0
UDP-Gal	+	Gal-α-Bz	↔	UDP	+	Gal-*-Gal-α-Bz	1.6
UDP-Gal	+	Gal-β-Bz	↔	UDP	+	Gal-*-Gal-β-Bz	3.6
UDP-Gal	+	Gal-β1,4-Xyl-β-Bz	↔	UDP	+	Gal-*-Gal-β1,4-Xyl-β-Bz	7120
UDP-glucose	+	Gal-β1,4-Xyl-β-Bz	↔			No product	0
UDP-xylose	+	Gal-β1,4-Xyl-β-Bz	↔			No product	0
UDP-GalNAc	+	Gal-β1,4-Xyl-β-Bz	↔			No product	0
Proteoglycan tetrasaccharide linker						GlcA-β1,3-Gal-β1,3-Gal-β1,4-Xyl-1β-O-serine-(protein)	

[a] All reaction rates reflect the activity of 7.8 pmol of pure recombinant Y110A2AL.14 protein.

devoid of fluorescence and the pattern of anti-Gal-T2 scFv antibody fluorescence is similar to that seen with other examples of worm Golgi proteins (Chen *et al*., 1999). Therefore, anti-Gal-T2 antibody staining suggests that early embryos are loaded with maternal Gal-T2 protein. The perinuclear staining pattern detected by the antibody was similar to the detection of a Gal-T2::GFP transgene reporter, in which the first 60 amino acids of Gal-T2 (including the N-terminal transmembrane domain and stem region) was fused to the N terminus of GFP. This reporter is designed to replace the Gal-T2 catalytic domain with GFP (Figure 4, D and E). The transgene reporter is expressed at a low level in intestinal cells, showing diffuse staining that is concentrated adjacent to the nucleus (Figure 4D).

To determine whether the antibody was against the Gal-T2 protein and not the recombinant tags or putative *N*- or *O*-glycan side chains, we used Western blot analysis against recombinant and deglycosylated Gal-T2 protein preparations (Figure 4F). ELISA and Western blot analysis showed that the antibody recognized a recombinant Gal-T2 (31–330-aa) protein preparation, lacking the purification tags (our unpublished data). Under nonreducing conditions in SDS-PAGE, recombinant Gal-T2 migrates almost mainly as a dimer (our unpublished data), whereas on a reducing denaturing gel Gal-T2 migrated as a 40-kDa monomer, with a weak 76-kDa dimer band (Figure 4F). Sequence analysis shows that Gal-T2 has two potential *N*-glycosylation sites and a putative mucin domain in the stem region (position 31–71), which has 46% serine + threonine + proline content. Gal-T2 is itself a glycoprotein, as combined *N*-glycanase and *O*-glycanase treatment resulted in a mobility shift (Figure 4F, lane 3 and 4). The formation of Gal-T2 dimers is consistent with other galactosyltransferases (both β1,3 and β1,4 galactosyltransferases), which also form dimers (Yamaguchi and Fukuda, 1995; Ju *et al*., 2002). The combined antibody and GFP data support the interpretation that Gal-T2 is a Golgi protein, localized in a perinuclear pattern in early stage embryos.

First and Second Generation RNAi Knockdown Phenotypes for Gal-T2

To further understand the loss-of-function phenotype of glycosyltransferases in the proteoglycan pathway, Gal-T2 RNAi was performed for one or two generations. The F_1 phenotype of Gal-T2 dsRNA injected animals was variable, with many injection experiments yielding wild-type F_1 embryos. When multinucleated embryos occurred, a high percentage of the F_1 siblings shared this lethal defect in cytokinesis. This suggested that RNAi lowered the expression of Gal-T2 mRNA or protein in some of the injected mothers to a critical or lower threshold level before the lethal phenotype predominated. Quantitative reverse transcription-PCR (Q-RT-PCR) indicated that a 18-fold reduction in Gal-T2 mRNA resulted in the arrested embryos relative to wild-type embryos (Figure 5A). Q-RT-PCR of staged embryo and larval preparations also showed that Gal-T2 is present at all stages of development and up-regulated in early adulthood, during egg laying (Figure 5B).

To deplete maternal and zygotic Gal-T2 mRNA and protein, RNAi treatment was extended for two generations, by feeding with bacterial strains engineered to express Gal-T2 dsRNA. Lactose plates were used for RNAi treatments, because they were significantly more effective than IPTG plate induction. Both the ppXyl-T and Gal-T2 RNAi feeding phenotypes were identical to each other (Figure 5, C, D, and F). On lactose plates, bacterial feeding RNAi produced a strong phenotype; however, lactose feeding plate phenotypes were not as variable as seen with the injected animals. The P_0 animals, fed on Gal-T2 lactose-RNAi plates, seemed normal and produced viable F_1 offspring, regardless of whether the P_0 were seeded on RNAi plates as L1 or L4 larva. Typically, RNAi feeding of L1 larva is sufficient for depletion of adult mRNA, whereas RNAi feeding of L4 larva has an immediate knockdown of early embryonic mRNA. Embryonic arrest was virtually absent in the F_1 generation from P_0 RNAi animals. However, when these RNAi-treated F_1 offspring were transferred to fresh RNAi lactose plates (for a second generation of RNAi feeding), they developed to F_1 adults that fed well, exhibiting strong pharyngeal pumping, but did not move. These F_1 adults were small, clear, and slightly egg-laying defective, with a uterus bloated with embryos. Greater than half of F_1 adults had their uterus completely filled with cytokinesis-deficient embryos of various sizes (Figure 5D). Nearly 100% of the F_2 embryos laid by these adults also lacked cell membranes and had unusual egg shapes. Therefore, either RNAi depletes maternal Gal-T2

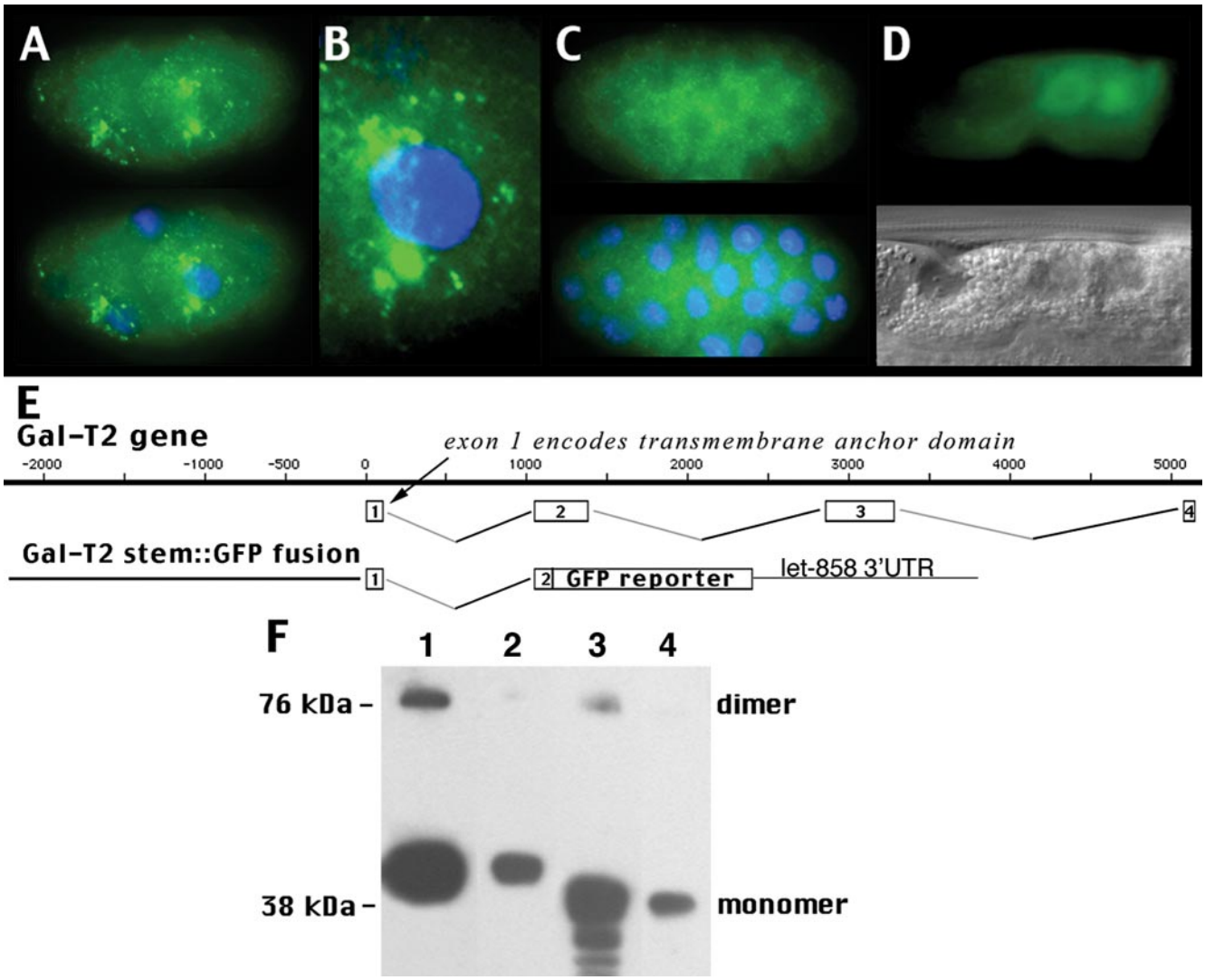

Figure 4. Gal-T2 localization and detection in *C. elegans*. (A) Anti-Gal-T2 scFv antibody staining alone (top) or with DAPI nuclear counterstain (bottom) in an eight-cell embryo. (B) High magnification of Golgi apparatus staining and nuclei from embryo in A. (C) Anti-Gal-T2 scFv antibody staining in a 28-cell embryo shows perinuclear staining pattern. (D) GFP fluorescence staining and DIC of intestinal cells from transgenic animals expressing a fusion of the N terminus and stem of Gal-T2 (1–60 aa) to a GFP reporter. Two nuclei are present in the GFP-positive cell. The GFP fluorescence surrounds the left nucleus and forms a patch next to the right nucleus. The nuclei themselves do not exhibit a GFP signal. (E) Structure and design of the wild-type Gal-T2 gene and the Gal-T2 stem::GFP reporter. GFP is fused to amino acid codon 60 in the second exon, such that GFP replaces the C-terminal catalytic domain of Gal-T2. (F) Western blot detection of Gal-T2 with anti-Gal-T2 scFv antibody. Lanes 1 and 2, 50 and 20 ng of recombinant Gal-T2, lacking the N-terminal transmembrane domain. In place of the transmembrane domain, a 38-amino acid purification tag is genetically fused to the stem and catalytic domain of Gal-T2 (see *Materials and Methods* for details). Lanes 3 and 4, 40 and 15 ng of recombinant Gal-T2 after peptide:N-glycanase and *O*-glycanase treatment.

protein after a sufficient period of RNA degradation or the RNA degradation phenomenon increases in amplitude after extensive RNAi treatment.

To examine the Gal-T2 RNAi phenotype for nuclear division in the absence of cytokinesis (the cytokinesis defect), F_2 embryos were treated for 2 min with the fluorescent dye DAPI, which does not penetrate normal embryo membranes. These DAPI-treated F_2 embryos were permeable, staining positive for multiple nuclei, suggesting a deficiency both in the eggshell and cell membranes. Although no new cell membranes formed, nuclei continued to divide for four or five rounds of division, because typically ~20 nuclei were present in the arrested embryos (Figure 5E). Nuclei clumped together in one or more locations, which only occurs when the cellularization is absent. This Gal-T2 RNAi feeding phenotype is essentially identical to the phenotype observed for ppXyl-T in histone::GFP tagged animals (Figure 2A). Although multinucleated embryos were visible on the Gal-T2 RNAi lactose plate by differential interference contrast (DIC) or brightfield microscopy (Figure 5F), most of these embryos rapidly lost their multinucleated appearance and began to degrade, resulting in embryos looking like those in Figure 5, E and G. DIC microscopic examination of the F_1 adults from second generation feeding also showed that many embryos were fertilized in utero, but began degrading before being laid. F_1 adults had a very short life span, because all second generation RNAi-treated animals died prematurely at 6 d postfertilization. Wild-type animals and first generation RNAi-treated animals had a normal life span, >2 wk.

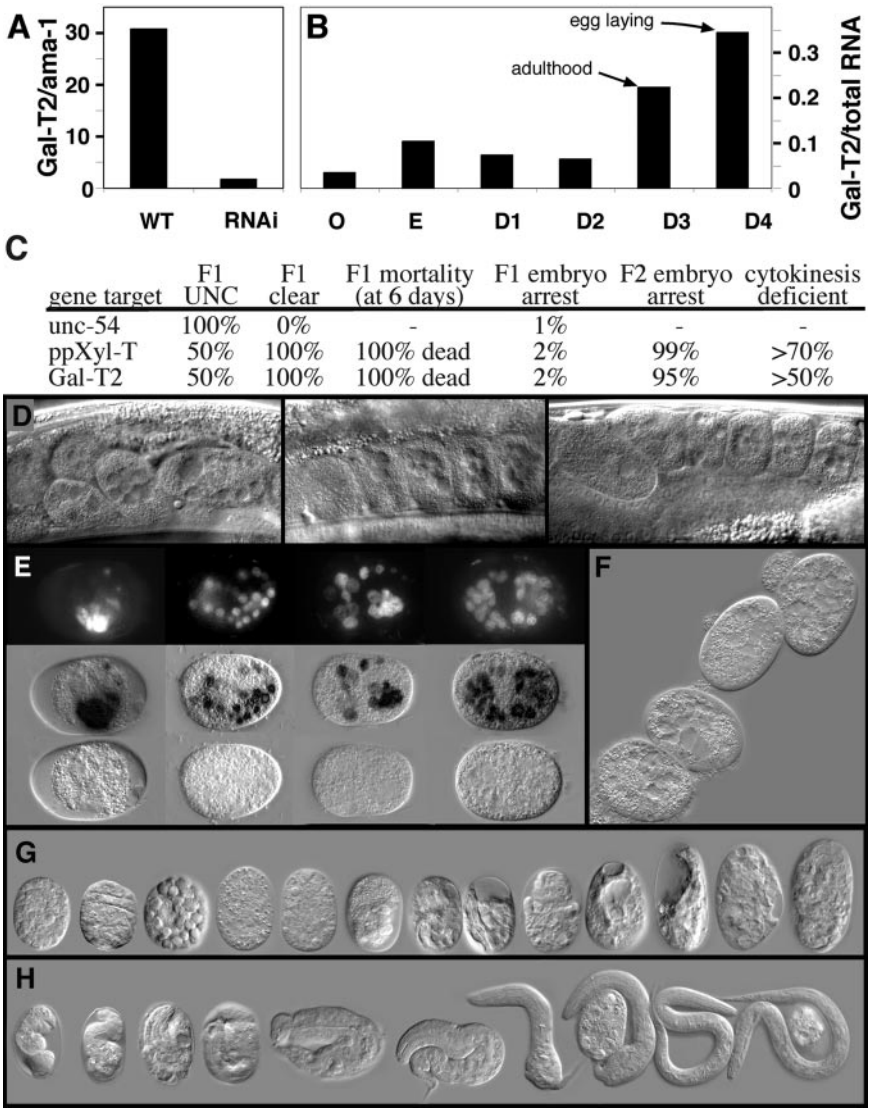

Figure 5. Gal-T2 depletion impairs embryonic development. (A) Quantitative reverse transcription-PCR on wild-type and Gal-T2 RNAi-treated embryos shows a 18-fold reduction in Gal-T2 mRNA. RNA levels from 20 embryos in the two preparations are normalized against an *ama-1* control mRNA. (B) Q-RT-PCR of Gal-T2 message from the following staged *C. elegans* RNA preparations: oocytes, embryos, day 1 (L1) larva, day 2 (L2/L3) larva, day 3 (L4 larva and young adults), and day 4 (gravid adults). Identical quantities of total RNA from each staged preparation are used in Quantitative RT-PCR. (C–F) Induction of Gal-T2 RNAi on lactose plates. (G and H) Induction of Gal-T2 RNAi on IPTG plates. (C) Bacterial feeding RNAi at 23°C on lactose plates for two generations. Cytokinesis defects were examined in the embryos laid on the plate and also while embryos were still in the uterus of gravid adults. (D) The uterus of three gravid adults from first generation Gal-T2 lactose-induced RNAi plates show multi-nucleated embryos, variation in egg size, and degrading embryos. (E) Embryos from second generation Gal-T2 lactose-induced RNAi plates. Bottom, DIC of the most common embryos after two generations of RNAi. Top, DAPI staining of nuclei. Middle, merges the DAPI stain (converted to black) over the DIC image. (F) Multinucleated embryos from second generation of RNAi feeding on lactose plates are deficient in cytokinesis. After a few hours, these multinucleated embryos begin to degrade and resemble embryos shown in Figure 4, E and G. (G) Egg size and shape defects and embryonic arrest in second generation of Gal-T2 RNAi treatment on IPTG plates. (H) Gal-T2 RNAi also produces partially developed embryos and larva, displaying a shortened or NOB (no backside) phenotype on IPTG plates.

A second generation of bacterial feeding RNAi treatment also was evaluated on IPTG plates, because this is the traditional method used in genome-wide screens. IPTG-induction of RNAi, however, led to only a 54% embryonic arrest rate in F_2 offspring. The first or second generation lethality rates on IPTG plates did not increase with the use of an RNAi hypersensitive *rrf-3* mutant strain (our unpublished data). Furthermore, the IPTG-induced phenotype had lower penetrance, as embryos exhibited different sizes and shapes, relative to wild-type controls, but arrested at different stages of development (Figure 5, G and H). Among those F_2 that did hatch, significant abnormalities in body morphology were apparent, primarily a shorter body plan or a Nob (no backside) phenotype (Figure 5H). This intermediate phenotype, therefore, provides a means to study the requirement of proteoglycans at later stages of development.

DISCUSSION

The majority of the genes that initiate protein glycosylation reactions do not seem to be essential for the completion of cytokinesis. Genes in the proteoglycan biosynthesis pathway seem to have a unique role in early embryo cytokinesis. RNAi knockdown of ppXyl-T or Gal-T2 resulted in a cytokinesis defect, which seemed identical to strong mutations in the chondroitin synthase gene *sqv-5* (Hwang *et al*., 2003b; Mizuguchi *et al*., 2003). Embryos and animals that escaped one or two generations of ppXyl-T or Gal-T2 RNAi treatment exhibited later stage embryonic arrest, abnormal larva, and adult anatomy and premature death, which is similar to a heparan synthase *rib-2* null phenotype (Morio *et al*., 2003). Therefore, depletion of the proteoglycan linker tetrasaccharide (through ppXyl-T and Gal-T2 RNAi) will impact post-translational modification of both chondroitin and heparan proteoglycans. By comparing different RNAi methodologies on the glycosyltransferases in this study, it is clear that genome-wide RNAi screen studies need to be interpreted with caution because the traditional RNAi methodology (RNAi induction with IPTG plates for a single generation) did not produce a potent knockdown of glycosyltransferases.

The cytokinesis defect in ppXyl-T-deficient embryos was very specific. Early embryonic blast cells were able to initiate cytokinesis. However, at the terminal phase of cytokinesis,

cell membrane formation at the daughter-cell interface stalled and retracted, and the cells were flattened against the eggshell and lost their normal shape. It is possible that membrane vesicle transport on the spindle is still intact, because, in ppXyl-T RNAi-treated embryos, the spindle position, migration and rotation are normal for a few nuclear divisions (Figure 2). Furthermore, such cytokinesis-deficient embryos exhibited no defects in embryo polarity with respect to PIE-1 protein distribution. This ppXyl-T loss-of-function phenotype seemed similar to a brefeldin A-induced block in vesicle transport in *C. elegans* embryos, suggesting that the brefeldin A phenotype could be the result of blocking the delivery of proteoglycans to the membrane interface of newly dividing cells. (Skop *et al*., 2001).

Our initial RNAi screen probed multiple protein glycosylation pathways. When embryos were deficient in *N*-glycosylation machinery, cytokinesis also was impaired; however, the embryonic arrest phenotype was variable and less specific to cytokinesis. Inconsistent defects in *N*-glycosylation-deficient embryos are probably of pleiotrophic or secondary origin, because *N*-linked glycans are required for chaperone-assisted folding of large numbers of different structural proteins, enzymes and transporters. Therefore, an *N*-glycan-deficiency may indirectly impair proteoglycans, because most enzymes in the proteoglycan biosynthetic pathway are themselves *N*-linked glycoproteins.

It is not clear whether the proteoglycan-dependent terminal phase of cytokinesis is a generalized process that applies to all higher eukaryotic cell division events. Even in *C. elegans*, the multinucleated embryonic phenotype is primarily observed in the early embryo at the first or second cell cleavage, and rarely later. We did not detect significant occurrences of multinucleated cells after the four-cell stage. Also, the GAG chain chondroitin is present in fertilized eggs but is not specifically localized to cleavage furrows or to the newly dividing membrane plane (Mizuguchi *et al*., 2003). Therefore, it is likely that chondroitin may mediate overall cell membrane–extracellular matrix interactions to stabilize cell shape, which is important for forming a stable interface between newly dividing cells in the very early embryo. At later developmental stages, it is possible that cells recruit different species and classes of glycoproteins to stabilize existing cell membrane integrity, shape, attachment as well as stabilize newly forming cell membranes in daughter-cell cleavage planes. In mammals, glycoproteins are expressed in the cleavage plane of dividing cells, in a tissue and stage-specific manner. For example, some human leukocytes express and recruit the mucin glycoprotein CD43 at the cleavage furrow during cell division (Yonemura *et al*., 1993). Each CD43 molecule is a heavily glycosylated integral membrane protein with up to 90 mucin-type oligosaccharide chains on its extracellular domain. Mucin glycosylation may be important for cell division in some human leukocytes; however, there is no obvious role known for mucin glycosylation in the early *C. elegans* embryo, because RNAi of the nine polypeptide GalNAc transferases (ppGaNTases) did not reveal any cytokinesis defects or early embryonic arrest (Table 1). However, a role for these ppGaNTases in cell division may be masked by redundant isoforms that could be coexpressed in the embryo or gonads.

In summary, the terminal phase of cytokinesis in the early *C. elegans* embryo has a unique requirement for proteoglycan modification of the cell surface. This observation is consistent with the recent reports on the *sqv-5* gene, which indicates that an essential component of newly dividing cells is the extracellular matrix glycosaminoglycan chondroitin (Hwang *et al*., 2003b; Sugahara *et al*., 2003). To gain more insight into the role of proteoglycans in cell division, future studies should identify the core proteins modified with proteoglycans in oocytes and the early embryo. Also the role of sulfate modification of the chondroitin or dermatan GAG chains by sulfotransferases should be explored to help us understand how negatively charged sugar polymers stabilize the cell membranes during cytokinesis.

ACKNOWLEDGMENTS

We thank Yuji Kohara for cDNA clones; Keith Nehrke and Shona Mookerjee for initial cDNA library screening; the Caenorhabditis Genetics Center for N2 and NL2099 nematode strains; Andy Fire for the bacterial feeding vectors; Geraldine Seydoux and Eleanor Maine for sharing GFP-tagged nematode strains; and Robert Barstead for cDNA libraries. This work is supported by a Mizutanti Foundation and National Institutes of Health (DE14088-02) grants (to F.K.H.) and the Max Planck Society (to A. S.).

REFERENCES

Bateman, A., *et al*. (2004). The Pfam protein families database. Nucleic Acids Res. *32*, D138–D141.

Chen, S., Zhou, S., Sarkar, M., Spence, A. M., and Schachter, H. (1999). Expression of three *Caenorhabditis elegans N*-acetylglucosaminyltransferase I genes during development. J. Biol. Chem. *274*, 288–297.

Finger, F. P., and White, J. G. (2002). Fusion and fission: membrane trafficking in animal cytokinesis. Cell *108*, 727–730.

Gotting, C., Kuhn, J., Zahn, R., Brinkmann, T., and Kleesiek, K. (2000). Molecular cloning and expression of human UDP-d-Xylose:proteoglycan core protein β-d-xylosyltransferase and its first isoform XT-II. J. Mol. Biol. *304*, 517–528.

Hagen, F. K., Layden, M., Nehrke, K., Gentile, K., Berbach, K., Tsao, C. C., and Forsythe, M. (2001). Mucin-type *O*-glycosylation in *C. elegans* is initiated by a family of glycosyltransferases. Trends Glycosci. Glycotech. *13*, 463–479.

Hagen, F. K., and Nehrke, K. (1998). cDNA cloning and expression of a family of UDP-N-acetyl-D-galactosamine:polypeptide N-acetylgalactosaminyltransferase sequence homologs from *Caenorhabditis elegans*. J. Biol. Chem. *273*, 8268–8277.

Haidaris, C. G., Malone, J., Sherrill, L. A., Bliss, J. M., Gaspari, A. A., Insel, R. A., and Sullivan, M. A. (2001). Recombinant human antibody single chain variable fragments reactive with *Candida albicans* surface antigens. J. Immunol. Methods *257*, 185–202.

Hwang, H. Y., and Horvitz, H. R. (2002). The SQV-1 UDP-glucuronic acid decarboxylase and the SQV-7 nucleotide-sugar transporter may act in the Golgi apparatus to affect *Caenorhabditis elegans* vulval morphogenesis and embryonic development. Proc. Natl. Acad. Sci. USA *99*, 14218–14223.

Hwang, H. Y., Olson, S. K., Brown, J. R., Esko, J. D., and Horvitz, H. R. (2003a). The *Caenorhabditis elegans* genes sqv-2 and sqv-6, which are required for vulval morphogenesis, encode glycosaminoglycan galactosyltransferase II and xylosyltransferase. J. Biol. Chem. *278*, 11735–11738.

Hwang, H. Y., Olson, S. K., Esko, J. D., and Horvitz, H. R. (2003b). *Caenorhabditis elegans* early embryogenesis and vulval morphogenesis require chondroitin biosynthesis. Nature *423*, 439–443.

Jantsch-Plunger, V., and Glotzer, M. (1999). Depletion of syntaxins in the early *Caenorhabditis elegans* embryo reveals a role for membrane fusion events in cytokinesis. Curr. Biol. *9*, 738–745.

Ju, T., Cummings, R. D., and Canfield, W. M. (2002). Purification, characterization, and subunit structure of rat core 1 β1,3-galactosyltransferase. J. Biol. Chem. *277*, 169–177.

Kamath, R. S., *et al*. (2003). Systematic functional analysis of the Caenorhabditis elegans genome using RNAi. Nature *421*, 231–237.

Knauer, R., and Lehle, L. (1999). The oligosaccharyltransferase complex from yeast. Biochim. Biophys. Acta *1426*, 259–273.

Krogh, A., Larsson, B., von Heijne, G., and Sonnhammer, E. L. (2001). Predicting transmembrane protein topology with a hidden Markov model: application to complete genomes. J. Mol. Biol. *305*, 567–580.

Mizuguchi, S., Uyama, T., Kitagawa, H., Nomura, K. H., Dejima, K., Gengyo-Ando, K., Mitani, S., Sugahara, K., and Nomura, K. (2003). Chondroitin proteoglycans are involved in cell division of *Caenorhabditis elegans*. Nature *423*, 443–448.

Morio, H., Honda, Y., Toyoda, H., Nakajima, M., Kurosawa, H., and Shirasawa, T. (2003). EXT gene family member rib-2 is essential for embryonic

development and heparan sulfate biosynthesis in *Caenorhabditis elegans*. Biochem. Biophys. Res. Commun. *301*, 317–323.

Nonet, M. L., Grundahl, K., Meyer, B. J., and Rand, J. B. (1993). Synaptic function is impaired but not eliminated in *C. elegans* mutants lacking synaptotagmin. Cell *73*, 1291–1305.

Ono, K., Parast, M., Alberico, C., Benian, G. M., and Ono, S. (2003). Specific requirement for two ADF/cofilin isoforms in distinct actin-dependent processes in *Caenorhabditis elegans*. J. Cell Sci. *116*, 2073–2085.

Piekny, A. J., and Mains, P. E. (2002). Rho-binding kinase (LET-502) and myosin phosphatase (MEL-11) regulate cytokinesis in the early *Caenorhabditis elegans* embryo. J. Cell Sci. *115*, 2271–2282.

Skop, A. R., Bergmann, D., Mohler, W. A., and White, J. G. (2001). Completion of cytokinesis in *C. elegans* requires a brefeldin A-sensitive membrane accumulation at the cleavage furrow apex. Curr. Biol. *11*, 735–746.

Straight, A. F., and Field, C. M. (2000). Microtubules, membranes and cytokinesis. Curr. Biol. *10*, R760–R770.

Sugahara, K., Mikami, T., Uyama, T., Mizuguchi, S., Nomura, K., and Kitagawa, H. (2003). Recent advances in the structural biology of chondroitin sulfate and dermatan sulfate. Curr. Opin. Struct. Biol. *13*, 612–620.

Timmons, L., Court, D. L., and Fire, A. (2001). Ingestion of bacterially expressed dsRNAs can produce specific and potent genetic interference in *Caenorhabditis elegans*. Gene *263*, 103–112.

Yamaguchi, N., and Fukuda, M. N. (1995). Golgi retention mechanism of β-1,4-galactosyltransferase. Membrane-spanning domain-dependent homodimerization and association with α- and β-tubulins. J. Biol. Chem. *270*, 12170–12176.

Yan, A., and Lennarz, W. J. (2005). Unraveling the mechanism of protein N-glycosylation. J. Biol. Chem. *280*, 3121–3124.

Yonemura, S., Nagafuchi, A., Sato, N., and Tsukita, S. (1993). Concentration of an integral membrane protein, CD43 (leukosialin, sialophorin), in the cleavage furrow through the interaction of its cytoplasmic domain with actin-based cytoskeletons. J. Cell Biol. *120*, 437–449.